Zero-Points of FOS Wavelength Scales

Michael R. Rosa [1,2], Florian Kerber [1,3], and Charles D.(Tony) Keyes[4]

[1)] Space Telescope European Coordinating Facility, European Southern Observatory, Garching, Germany

[2)] Affiliated to the Astrophysics Division, Space Science Department, European Space Agency

[3)] Institute for Astronomie, University of Innsbruck, Austria

[4)] Space Telescope Science Institute, Baltimore, MD

June 1998

ABSTRACT

The internal zero-points of the FOS on-orbit wavelength calibration between 1990 (launch, OV/SV) and 1997 (decommissioning) have been determined. The analysis is based on cross-correlating all WAVECAL exposures for the high-resolution dispersers and for the low resolution G650L mode (about 1200 data sets), using as templates those exposures which define the dispersion solutions currently in use by the FOS pipeline. For FOS/BL systematic shifts of the zero-points are present, which are very similar for all disperser and aperture combinations, and amount to a maximum offset of 7 pixels (1.75 diodes) over the entire period. The zero-points for FOS/RD present an apparently random distribution with a peak-to-peak range of 7 pixels (1.75 diodes). The shifts are provisionally attributed to the differing behavior of the two detectors in the geomagnetic field, as well as residual errors not compensated by the on-board GIM algorithm. We describe a corrective procedure which will restore a maximum 1 pixel peak-to-peak uncertainty in the wavelength scale to all FOS/BL high-resolution and G650L spectra. The information provided in this ISR will allow manual post-processing correction of the wavelength scale for FOS/BL data taken at any epoch; STSDAS/IRAF, IDL, and MIDAS scripts for correction of the wavelength scales are available for download on the STScI FOS WWW pages. The correction will also be implemented in **calfos***, once the FOS/RD data have been fully analyzed, so that routine re-calibration of FOS data will result in correct wavelengths. At the time of writing the corrective measures for FOS/RD data have not yet been determined and the effect of the wavelength correction for FOS/BL on instrumental sensitivities (flux calibration) is still under investigation.*

This report encompasses a variety of topics that are of interest to a broad spectrum of users. To help you find information, we list the major sections of this document:

1. Introduction

The FOS was designed primarily as a faint object spectrophotometer, with less stringent requirements on highly reproducible velocity measurements. As described in the FOS Instrument Handbook (all versions) there are unavoidable intrinsic errors in the wavelength scale zero-points, mainly due to non-repeatability in the settling of the rotating filter-grating wheel assembly (FGWA). Additional uncertainties arising from non-optimal centering of point sources, and the offsets between internal (calibration lamp) and external sources, are discussed in the FOS section (primarily chapter 32) of the HST Data Handbook, volume II.

Preflight experiments showed that the non-repeatability of the grating wheel could be limited to a few pixels (fraction of a diode) by forced overstepping and rewinding (FOS ISR CAL/FOS 60), a procedure finally adopted for on-orbit operations. On-orbit analysis indicated that the total 1 σ error budget of grating wheel non-repeatability, source miscentering and internal to external wavelength scale offsets should not exceed 2 pixels (0.5 diodes or approximately 0.25 resolution elements) (cf HST Data Handbook). In addition, dispersion relations fitted to calibration lamp exposures regularly obtained for monitoring purposes did not directly show any obvious trends. Therefore, the original set of dispersion solutions, which were a product of the science verification (SV) activity, was used throughout the entire operational life of FOS as the default in the pipeline calibration.

Observers planning to use FOS data for radial velocity studies were routinely advised to obtain their own dedicated wavelength calibration observations contemporaneous with the science exposures in a sequence without aperture or grating wheel movements. An analysis of the FOS exposure catalogue shows that very few FOS observations were actually obtained in this manner.

Lately, indications have been accumulating that FOS wavelength scale zero-points might occasionally be much more in error than the fractional diode figure given above. Among these are irregularities in other calibration quantities such as flux scale and Y-base that could only be explained by X-drifts, inquiries by GOs facing mismatches between the radial velocities obtained from FOS data when compared to ground based data, and a detailed analysis of FOS radial velocity data sets by van der Marel (1997).

In conjunction with the ST-ECF FOS Post Operational Archive project, and as part of the ongoing STScI and ST-ECF support of FOS archival data, calibration, and users, we have reanalyzed all FOS wavelength calibration observations ever obtained on-orbit. Results are presented and discussed in this report.

2. Analysis Method

Usually the FOS dispersion calibration exposures have been analyzed by fitting dispersion solutions to the line positions of catalogue wavelength standards and then comparing the 3rd order polynomial coefficients. This process should in principle detect changes in both the slope and the zero-point of the wavelength scale. However, because of masking between the 4 coefficients involved, subtle changes, especially in the zero-points are subject to dilution and do not fully project into the zero-order coefficient. We therefore chose to cross-correlate the raw, uncalibrated exposures, covering the entire period between OV/SV (August 1990) and the last on-orbit wavelength calibration observation obtained in December 1996 (FOS was decommissioned on 13 February 1997) with a single template for each FOS disperser respectively. The template raw calibration lamp exposures are those used for the SV dispersion analysis (FOS ISR CAL/FOS 67) which define the default dispersion relations used throughout by the FOS pipeline (see Table 1, which is a revised version of Table 1 from FOS ISR CAL/FOS 67; our revisions correct minor aperture and disperser nomenclature errors found in the original).

Cross-correlation of the data sets yields a very clean peak which can be positioned to better then 0.1 pixel (3 sigma) using gaussian profile fitting for all high and low dispersion gratings. Due to the sparsity of unblended lines in the data for PRISM and G160L, results for these dispersers are much less accurate and indicative only (see discussion).

Although this analysis is primarily aimed at finding zero-point shifts, and FOS dispersion calibration monitoring showed that the wavelength scales (slopes) remained stable, we performed a partial test for slope changes on several datasets by windowing the pixel array into 3 equally long sections. The offsets obtained in these 3 subwindows do agree within the measuring uncertainty. These tests do not provide a rigorous basis for the exclusion of slope changes over the lifetime of the FOS, however. In the following we report on results obtained from the shift averaged over the full pixel arrays.

Throughout the paper we report shifts in the sense

$$\Delta x = x(\text{template}) - x(\text{data}), \qquad \text{Eq. 1}$$

such that a negative Δx is obtained if a spectral feature seen at a given pixel x in the template is found at a higher pixel number ($x-\Delta x$) in the data under question.

3. Results

General findings

For the analysis we broke down the samples according to detector, grating and aperture, and plotted the x-shifts versus the Modified Julian Date (MJD) of exposure start. As opposed to expectations (see introductory background information above), substantial shifts were found for all FOS dispersers, over both short and long time intervals, amounting to a full amplitude variation of 7 pixels peak-to-peak on both FOS channels (see Figure 1). On the other hand, close inspection of sequences of exposures taken with the same disperser and no movement of the FGWA do have very similar shifts, which smoothly evolve in time at a scale of roughly only 0.1 pixel per HST orbit (two such sequences are shown in the upper panel of Figure 2).

Moving the filter-grating wheel between exposures in the same sequence can introduce shifts of +/- 1 pix, particularly well seen in sequences of wavelength calibration exposures followed by an ACQ IMAGE (spectral element MIRROR) and then science exposures with associated wavecals (Figure 2 - middle panel). Hence the recommendations of various FOS Instrument Handbooks are borne out as *a science observation without special wavecals, but close in time to an applicable wavecal, may still suffer from a substantial wavelength uncertainty*. On the other hand, changing apertures on the wavecal source does not introduce shifts of more than 0.2 pixel (see lower panel of Figure 2), in agreement with expectations and the results of FOS ISR CAL/FOS 131.

FOS/BL specific:

All the FOS blue side dispersers show a very similar and conspicuous pattern with time (cf. Figure 1). At any given epoch the peak-to-peak scatter of the zero-point offset about the mean trend is approximately +/- 1 pixel (i.e. 10 times the measurement error). The general trend amounts to an average drift of 0.75 pix/year with respect to the zero-point of the pipeline wavelength scale for each disperser. An observation in Cycle 6 therefore might be off by more than 5 pixels from nominal (~300 km/sec for the high resolution dispersers, ~1400 km/sec for low resolution G160L and ~4000 km/sec for little-used G650L).

Due to the apparent similarity in the pattern for all blue dispersers we combined all FOS/BL high-resolution and G650L grating data into a common dataset, depicted in Fig-

ure 1. This was done iteratively. A first straight combination, very similar to Figure 1, was used to define three windows in time, in which the data appear to follow different linear trends. Interestingly enough, the boundaries of these windows coincide with the start of OV/SV, the activation of on-board GIM correction, the installation of COSTAR and the decommissioning of FOS. The gap between MJD 48500 and 49000 corresponds to the epoch where the geomagnetically induced image motion problem (so-called GIM or GIMP) was known, but no on-board correction was then available. No wavecal observations were scheduled during this time interval. Linear regressions were fit to the data in these 3 windows, and were subsequently used to renormalize the shifts for each grating/aperture combination. The additive renormalization usually was less then 0.2 pix, except for the G270H (0.5 pixels) and the G570H (0.6 pixels) cases.

The renormalized data of all modes were finally recombined into a common data set, shown in Figure 1, and used to define the final three linear regressions (Table 2 and Table 3).

There are no apparent slopes in the residuals (average trend - individual disperser), reassuring that this procedure is valid. The grating-specific offsets, B_{gr} (see Table 3), which are effectively the FGWA-offsets of the initial epoch observations from the mean of the entire dataset, are found to be the same within the error margins in all 3 time windows. The scatter about the linear trend segments for each disperser is of the order of +/- 0.5 pixels, except for grating G270H (0.7 pixels).

The information in Table 2 and Table 3 forms the basis to compute expected offsets or zero-point corrections respectively, in the sense that:

(1) $\Delta x = A0 + A1*MJD(days) + B_{gr}$ [pix]

and

(2) x(true) = x(observed at MJD) + Δx (of MJD)

where x(true) is the x-position at which a spectral feature would have been observed if no shift had been present.

Figure 3 depicts the zero-point correction of all FOS/BL G400H wavecal datasets using this script.

FOS/RD specific:

The red side data points appear to present a scatter-diagram with no obvious trends in time and with a full peak-to-peak range of about 7 pixels. Separation of the data into sequences spanning only multi-orbit observations on the same target does, however, reveal interesting trends, such as depicted in the upper and lower panels of Figure 1 (see

previous discussion). In this report we can not offer a procedure that would easily recover the inherent 7 pixel (full amplitude) or 2.5 pixel (most likely value) uncertainty for any FOS/RD observation that was not immediately (i.e. within a fraction of the orbit) preceded or followed by a wavecal without any FGWA movement (see discussion below).

4. Discussion

All results strongly indicate that the main physical source of the problem of shifts in the x-scale (wavelength zero-point shifts) of FOS data is unrelated to either the aperture or the FGWA. It does seem to be a detector-related process instead. We offer the following hypothesis.

The long-term drift (see both panels of Figure 1) and short-term, orbital-position-related motion of the x-scale on the FOS diode arrays is very likely related to the differing magnetic shielding properties of the FOS Digicons, i.e., another incarnation of the GIM. FOS/BL, which had a factor 4-7 better mu-metal shield then FOS/RD, was not very susceptible to x-drifts as HST moved through its orbit. However, the shield could have acquired its own field over time, producing the long-term linear drifts. While the reversion of the direction after on-board GIM may be explained by the concomitant change in operational procedure regarding regular “degaussing”, we do not have an explanation yet for the resumption of the general trend after the first servicing mission. One possibility might be the change in ambient magnetic environment with the removal of HSP and the installation of the almost empty COSTAR container.

The FOS/RD Digicon detector assembly had an almost non-existent geomagnetic shield due to the loss of shielding capability of its mu-mantle during the installation process (FOS ISR CAL/FOS 98). The permeating geomagnetic field thus drove the spectral image around on the receiving diode array. In April 1993 the on-board GIM algorithm was implemented, using a simple geomagnetic field model and HST orbital parameters to anticipate this movement, to counteract it by adjusting voltages on deflection coils. According to the description in FOS ISR CAL/FOS 98, this algorithm assured against the relative movement from where an exposure started, but was never designed to reset the location at the start of the exposure to a “Zero-Field” reference point or the like.

The large scatter in the FOS/RD data therefore reflects the possible spread of starting locations from such a virtual reference position. In addition, the on-board GIM did not take into account the orientation of the spacecraft, hence the projection of the B-Field vector onto the FOS/RD Digicon. We thus see a residual movement of order 0.1 to 0.5 pixels as HST moved through the field while pointing to the same target on sequential exposures (see Figure 2 and van der Marel, 1997).

5. Corrective Measures

FOS/BL:

Rapid recovery script for GOs

The relations given in this report should enable GOs to shift their "c0" pixel/wavelength arrays, thereby recovering the +/- 1 pixel uncertainty level, which is about the level imposed by unrecoverable factors such as FGWA non-repeatability and internal/external offset. Below we indicate the logical steps to be taken. Working STSDAS, IDL, and MIDAS implementations of the procedure will be made available on the FOS WWW pages.

```
#############################################################################
# Script logic to work on dataset 'rootname':
#
#   make a safety backup copy of 'rootname'.c0h/d
#
#   produce a 2 column table 'work.tab'
#   fill column 1 ('pixel') with pixel index
#   copy current wavelengths (pixel values in 'rootname.c0d' into
#     'work.tab', column 2 ('wave_old')
#
#   determine the slope of the dispersion relation, (delta(wave)/delta(pix)),
#     e.g., by linear regression to columns 'pixel' and 'wave_old'
#
#   calculate predicted pixel shift:
#    1) get MJD of exposure (descriptor FPKTTIME in 'rootname'.c0h)
#    2) obtain from table 2 the parameters A1,A0 for the pixel shift correction
#       appropriate for the MJD of 'rootname' observation.
#    3) obtain from table 3 the grating specific offset B_gr for the
#       appropriate disperser (descriptor FGWA_ID in 'rootname'.c0h)
#    4) shift (pix) = A0 + A1*MJD + B_gr (preserve signs of parameters !)
#    5) shift (lambda[A]) = shift(pix) * delta(wave)/delta(pix)
#
#   compute the corrected dispersion solution 'wave_new' in table 'work.tab':
#       'wave_new' = 'wave_old' + shift(lambda)
#
#   overwrite the old wavelengths in 'rootname.c0d' with the
#      corrected values from 'work.tab' (columns 'pixel' and 'wave_new')
#
#   From this point onward the corrected wavelength scale is available by
#     default to the data analysis stream
#############################################################################
```

FOS/RD:

Use of a more sophisticated (e.g., 16 pole) geomagnetic field model in combination with the magnetometer readings from the telemetry stream and inclusion of the orientation of HST may allow us to devise a corrective algorithm for FOS/RD observations as well. Work continues on this possibility and will be reported in a forthcoming ISR.

Upgrading of CALFOS pipeline:

Naturally, a more sophisticated algorithm that is included in the FOS pipeline (**calfos**) will be able to correct the wavelength scale more accurately than the quick fix procedures above. The FOS pipeline will be upgraded to correct the wavelength scale once the analysis for both FOS/BL and FOS/RD is complete and a determination of the ideal update correction mechanism can be made. Ideally the pipeline should be fed with entirely new reference files for dispersion solutions and inverse sensitivities. Recall that the flux standard star exposures suffer from the same zero-point drifts. The maximum shift observed amounts to 7 pixels, and therefore we do not expect that significant errors occurred in the determination of the inverse sensitivities, *except for spectral regions where the sensitivity changes very rapidly*. The latter may be the range shortward of Lyα in G130H (FOS/BL), the blue end of G190H (FOS/RD), for both detectors the blue end of G160L and PRISM data, and the red end of G780H (FOS/RD).

For those who wish to address only the wavelength scale, several solutions are possible, but the most straightforward way is the quick solution script. The **calfos** algorithm works on pixel scales throughout and uses the dispersion solutions solely to produce an output wavelength array, the “c0” file.

One exception to this pixel-based methodology is the algorithm which windows-out bright sky lines in the sky background filtering option, but the shifts described here are insignificant in comparison to the window sizes. Additionally, we note that no FOS proposer chose sky subtraction as part of their planned science program activity; a few sky observations were obtained, but in all cases these observations were made due to program implementation error and they do not contribute to the science quality of the observation.

Before using the dispersion solution to create a wavelength array, **calfos** therefore could access a new reference table holding the information of Table 2 and Table 3, and compute a pixel shift accordingly. Rather then implementing a modified **calfos** now we will await the analysis of the FOS/RD shifts, so that both solutions can be implemented at one time. This is desirable because the FOS/BL and FOS/RD algorithmic solutions will almost certainly differ and so will the required reference data structures. By that time we should also have completed the analysis of the impact of the corrected wavelengths on the derived inverse sensitivities. In the interim, we encourage archival FOS users to utilize the formulae provided in this ISR or to download the scripts from the WWW in order to correct the wavelength scales of their FOS/BL data.

6. References

- Dahlem, M. and Koratkar, A., 1994, FOS ISR CAL/FOS 131 Post-COSTAR FOS Aperture Wheel Repeatability Measurements
- Fitch, J., Hartig, G., Beaver, E. and Hier, R., 1993, FOS ISR CAL/FOS 098 Correction of the geomagnetically induced image motion problem on the Hubble space telescope's Faint Object Spectrograph
- Hartig, G., 1989, FOS ISR CAL/FOS 060 FOS Filter-Grating Wheel Repeatability: Dependence on Motor Selection
- Keyes, T., ed., *HST Data Handbook*, volume II, 1997, STScI:Baltimore.
- Koratkar, A. and Evans, I.N., 1995, FOS ISR CAL/FOS 142 Repeatability of the FOS G130H Grating External Wavelength Zeropoint
- Koratkar, A. and Martin, S., 1995, FOS ISR CAL/FOS 145 FOS Filter-Grating Wheel Repeatability
- Kriss, G.A., Blair, W.P. and Davidsen, A.F., 1991, FOS ISR CAL/FOS 067 Revised FOS Wavelength Calibration
- Kriss, G.A., Blair, W.P. and Davidsen, A.F., 1992, FOS ISR CAL/FOS 070 Internal/External Offsets in the FOS Wavelength Calibration
- van der Marel, R.P., 1997, The HST/FOS Wavelength Scale in Calibrating HST with a New Generation of Instruments, ed., S. Casertano, R. Jedrzejewski, C. Keyes, and M. Stevens (STScI:Baltimore), p. 443

Table 1. FOS WAVECALs used to define the original pipeline wavelength calibration (revised version of Table 1 from FOS ISR CAL/FOS 67 with typographical errors corrected).

Dataset name	Detector	Disperser	Aperture	Dataset name	Detector	Disperser	Aperture
y0an0101	BLUE	G400H	0.1-PAIR	y0an0401	RED	G650L	0.1-PAIR
y0an0102	BLUE	G650L	0.1-PAIR	y0an0402	RED	G780H	0.1-PAIR
y0an0103	BLUE	PRISM	0.1-PAIR	y0an0403	RED	G270H	0.1-PAIR
y0an0104	BLUE	PRISM	0.1-PAIR	y0an0404	RED	G570H	0.1-PAIR
y0an0105	BLUE	G270H	0.1-PAIR	y0an0405	RED	G400H	0.1-PAIR
y0an0201	BLUE	G570H	0.25-PAIR	y0an0501	RED	G160L	0.25-PAIR
y0an0202	BLUE	G190H	0.25-PAIR	y0an0502	RED	PRISM	0.25-PAIR
y0an0203	BLUE	G130H	0.25-PAIR	y0an0503	RED	PRISM	0.25-PAIR
y0an0204	BLUE	G160L	0.25-PAIR	y0an0504	RED	G190H	0.25-PAIR
y0an0301	BLUE	G130H	0.3	y0an0601	RED	G400H	0.3
y0an0302	BLUE	G400H	0.3	y0an0602	RED	G160L	0.3
y0an0303	BLUE	G160L	0.3	y0an0603	RED	G650L	0.3
y0an0304	BLUE	G650L	0.3	y0an0604	RED	PRISM	0.3
y0an0305	BLUE	PRISM	0.3	y0an0605	RED	PRISM	0.3
y0an0306	BLUE	PRISM	0.3	y0an0606	RED	G780H	0.3
y0an0307	BLUE	G270H	0.3	y0an0607	RED	G270H	0.3
y0an0308	BLUE	G190H	0.3	y0an0608	RED	G190H	0.3
y0an0309	BLUE	G570H	0.3	y0an0609	RED	G570H	0.3

Table 2. Linear wavelength zero-point drift parameters for FOS/BL

Epoch	approx MJD	Calendar Date	A0	error (A0)	A1	error (A1)	scatter-amplitude
OV to onboard-GIM	48167-49083	April 1990 through 5 Apr 1993	+106.57	(0.41)	-0.00221	(0.00013)	+/- 0.4
onboard-GIM to COSTAR-insert	49084-49335	6 April 1993 through 10 Dec 1993	-115.44	(0.48)	+0.00231	(0.00089)	+/- 0.5
COSTAR to SM2	49336-50500	11 Dec 1993 to 13 Feb 1997	+60.14	(0.49)	-0.00126	(0.00009)	+/- 0.5

Table 3. FOS/BL grating-specific pixel offsets, B_{gr}, from linear zero-point drifts

Disperser	G130H	G190H	G270H	G400H	G570H	G650L	G160L	PRISM
Offset (B_{gr})	-0.817	+0.587	+0.081	-0.440	+0.080	-0.579	(0)	not allowed

Note: Offsets for G160L and PRISM are defaulted to 0.0, not measured because of noise. Quick-fix procedures will not update PRISM wavelengths, but will allow time-dependent updates to G160L with no additional grating-specific offset.

Figure 1: Measured cross-correlation offset in pixels between individual WAVECALs and pipeline-defining epoch WAVECAL, as defined in Eq. 1 of the text. Upper panel: FOS/BL high-resolution dispersers. Lower panel: FOS/RD high-resolution dispersers.

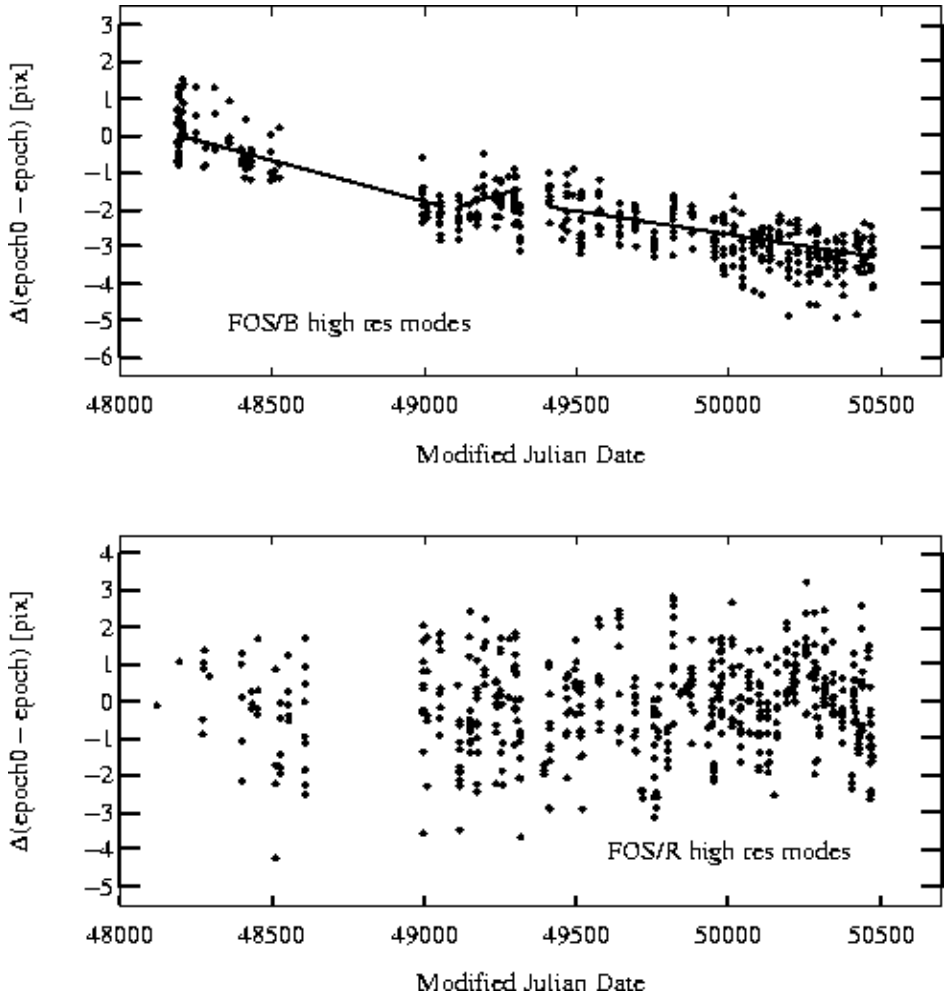

Figure 2: FOS/RD G570H short-term WAVECAL exposure sequences. Upper panel: two multi-orbit exposure series separated by a normal target acquisition. Middle panel: two sequences obtained on the same guide stars, but separated by FGWA motion to obtain a camera MIRROR image of the field. Lower panel: two sequences separated only by an aperture change from 0.1-PAIR to 0.25-PAIR.

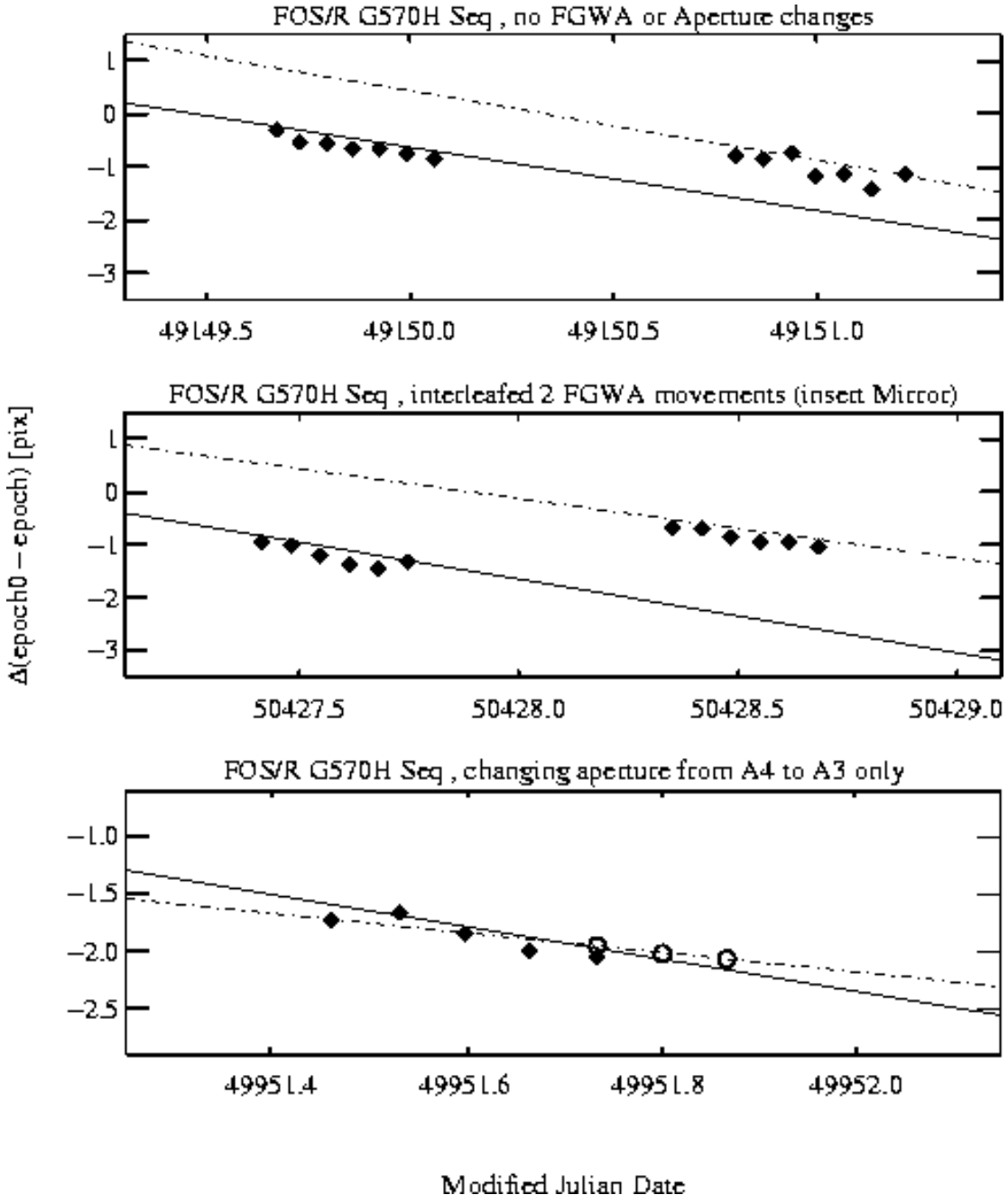

Figure 3: Filled symbols indicate mean offsets between WAVECALs and pipeline-defining WAVECAL as a function of date for FOS/BL G400H. Open symbols are the offsets after application of correction algorithm described in this report.